PROJECT 1 - 2023

Effect of Climate Change For Chicago and Miami

Group - 05

Project Report

SUBMITTED IN PARTIAL FULFILLMENT REQUIREMENT

FOR THE AWARD OF DEGREE OF

BACHELOR OF TECHNOLOGY

SUBMITTED BY

Deepanshu Aggarwal	220660
Radhika Bhati	220650
Sayantan	220590
Sejal Kumari	220586

UNDER THE SUPERVISION OF

Dr. Hirdesh Kumar Pharasi

SCHOOL OF ENGINEERING AND TECHNOLOGY

BML MUNJAL UNIVERSITY™
FROM HERE TO THE WORLD

BML MUNJAL UNIVERSITY Gurugram, Haryana - 122413 December 2023

CANDIDATE'S DECLARATION

We Deepanshu Aggarwal, Radhika Bhati, Sayantan, Sejal Kumari hereby declare that the project entitled ″Effect of Climate Change for Chicago and Miami" in fulfilment of completion of the 3rd-semester course –PRJ 1 as part of the Bachelor of Technology (B. Tech) program at the School of Engineering and Technology, BML Munjal University is an authentic record of our work carried out under the supervision of Dr. Hirdesh Kumar Pharasi. Due acknowledgments have been made in the text of the project to all other materials used.

This project was done in full compliance with the requirements and constraints of the prescribed curriculum.

Deepanshu Aggarwal

Sayantan

Radhika Bhati

Sejal Kumari

Place: Gurugram

Date: 21st December,2023

SUPERVISOR'S DECLARATION

This is to certify that the above statement made by the candidate is correct to the best of my knowledge.

Faculty Supervisor Name: Dr. Hirdesh Kumar Pharasi

Signature:

ABSTRACT

We look at the effects of climate change locally, specifically in Miami and Chicago, in our 13-year inquiry. Our investigation uses advanced visualization tools and thorough data examination, focusing on temperature, UV index, precipitation, and wind speed in these different metropolitan settings.

Finding related patterns, associations, and unique environmental trends that are common in Miami and Chicago is our main goal. This thorough analysis aims to provide priceless insights that cut across national borders, guiding decision-making in the areas of urban planning, policy creation, and climate adaption tactics.

The urgency to address climate change resonates vividly in both Miami and Chicago. Sustainable development in these urban areas hinges upon a profound understanding of the evolving climate dynamics and demands proactive, informed actions. Our analysis not only underscores this urgency but also endeavours to provide actionable, data-driven solutions crucial for steering both cities toward resilient and sustainable futures.

This initiative is a crucial call to action that highlights how important it is to address climate change in order to promote sustainable urban growth. It does this by using data-driven insights. Its ramifications go beyond these two cities and have an international impact, supporting a coordinated and proactive strategy for creating climate-resilient urban environments everywhere.

Keywords:

Climate Variability, Urban Resilience, Environmental Dynamics, Comparative Analysis, Data Visualization, Adaptive Strategies, Sustainable Development

ACKNOWLEDGEMENT

I am highly grateful to Dr. Hirdesh Kumar Pharasi, BML Munjal University, Gurugram, for providing supervision to carry out the Project from August -December 2022.

Dr. Hirdesh Kumar Pharasi has provided great help in carrying out our work and is acknowledged with reverential thanks. Without the wise counsel and able guidance, it would have been impossible to complete the training in this manner.

We would like to express thanks profusely to thank Dr. Hirdesh Kumar Pharasi, for stimulating me time to time. We would also like to thank entire team of BML Munjal University. We would also thank our groupmates who devoted their valuable time and helped me in all possible ways towards successful completion.

LIST OF FIGURES

TABLE OF CONTENT

Contents **Page No.**

Chapter – 1
INTRODUCTION

Welcome to our comprehensive project, "Climate Change Analysis in Miami and Chicago Over 13 Years. We dive into the complex tapestry of climate change impacts in this in-depth investigation. We concentrate on important environmental variables in these two different metropolitan environments, including temperature swings, variations in the UV index, precipitation patterns, and wind speed dynamics. Our focus spans critical environmental parameters such as temperature fluctuations, UV index variations, precipitation patterns, and wind speed dynamics in these two diverse urban landscapes.
Miami and Chicago's confluence in our analysis represents a dual viewpoint that enables us to draw conclusions from disparate but similar climates. We want to find patterns and connections between two physically separate but environmentally linked regions, in addition to individual city trends, by merging data from both cities.

Our basic objective is still the same: to unravel the complex narratives hidden in the data, illuminating the changing environmental landscapes of Miami and Chicago. This thorough investigation uses cutting-edge analytics, creative visualization approaches, and painstaking data processing to depict the subtleties of these various urban climates.

Combining data from Miami and Chicago offers a rare chance to compare, contrast, and possibly even create synergies between these two cities. Our goal is to investigate how climate change presents itself differently in these places, comprehending the common issues and applying the knowledge gained to guide decision-making procedures, urban planning techniques, and climate adaptation strategies.
As we navigate through the rich tapestry of data from Miami and Chicago, we hope to shed light on the past and open the door to a more resilient and sustainable future for urban landscapes dealing with the severe effects of climate change. Join us on this fascinating journey.

Chapter – 2
LITERATURE REVIEW

Title of paper	Author of paper	Summary
Comparison of NASA-POWER solar radiation data with ground-based measurements in the south of South America[1]	Facundo Orte, Facundo Carmona, Adan Faramiñán, Anabela Lusi, Raúl D'Elia, Elian Wolfram	The authors used data from five ground-based stations in Argentina to compare with the NASA-POWER data. They found that the NASA-POWER data overestimated global horizontal irradiance (GHI) by an average of 4.5%. However, the bias was higher in areas with high cloud cover, reaching up to 15%. The authors also found that the NASA-POWER data underestimated direct normal irradiance (DNI) by an average of 6.5%. However, the bias was lower in areas with high cloud cover. Overall, the authors found that the NASA-POWER data is a good resource for estimating solar radiation in the south of South America. However, they recommend using caution in areas with high cloud cover.
Evaluation of Satellite-Based, Modeled-Derived Daily Solar Radiation Data for	Jeffrey W. White, Gerrit Hoogenboom, Paul W. Wilkens, Paul W. Stackhouse Jr.,	The authors used data from 16 ground-based stations in the United States to compare with the satellite-based, modeled-derived data. They found that the satellite-based data overestimated global horizontal irradiance (GHI) by an average of 5.0%. However, the bias was higher in areas with

the Continental United States[2]	and James M. Hoel	high cloud cover and complex terrain, reaching up to 20%. The authors also found that the satellite-based data underestimated direct normal irradiance (DNI) by an average of 6.0%. However, the bias was lower in areas with high cloud cover and complex terrain. Overall, the authors found that the satellite-based, modeled-derived daily solar radiation data is a good resource for estimating solar radiation in the continental United States.
NEAR REAL-TIME GLOBAL RADIATION AND METEOROLOGY WEB SERVICES AVAILABL FROM NASA[3]	William S. Chandler, James M. Hoell, David Westberg, Charles H. Whitlock, and Taiping Zhang	This paper describes NASA's near real-time global radiation and meteorology web services. These services provide access to a variety of solar radiation and meteorological data products, including global horizontal irradiance (GHI), direct normal irradiance (DNI), and diffuse horizontal irradiance (DHI). The services are based on data from a variety of sources, including satellites, ground-based stations, and numerical weather models. The data is available at a variety of spatial and temporal resolutions, including hourly, daily, and monthly data. The services are a valuable resource for a wide range of applications, including solar energy forecasting, weather forecasting, and climate research.

Chapter – 3
OBJECTIVES

Our project's goals for analysing climate change in Miami and Chicago are as follows:

1. Evaluative Comparison: Analyse temperature, UV index, precipitation, wind speed, and other climate data from Miami and Chicago over the previous 13 years in detail to find trends that are similar, different, and related.

2. Pattern Identification: Apply cutting edge data analysis methods to identify patterns, trends, and unique environmental trends unique to every city in order to ascertain how climate change presents itself in these heterogeneous urban environments.

3. Educated Choice-Making: Provide insightful information from the comparative analysis to help Miami and Chicago make decisions about urban planning, policy, and other initiatives that will address climate change and promote sustainable development.

Chapter – 4
DESCRIPTION OF DATA

The list of parameters that are used in our dataset to describe the Earth's surface and atmosphere. The parameters are:

1. ALLSKY_SFC_UV_INDEX (CERES SYN1deg All Sky Surface UV Index): This parameter measures the intensity of ultraviolet (UV) radiation at the Earth's surface. UV radiation is a type of electromagnetic radiation that can damage DNA and cause skin cancer.

2. ALLSKY_SFC_UVB (CERES SYN1deg All Sky Surface UVB Irradiance): This parameter measures the amount of UVB radiation reaching the Earth's surface. UVB radiation is the type of UV radiation that is most responsible for skin cancer.

3. ALLSKY_SFC_UVA (CERES SYN1deg All Sky Surface UVA Irradiance): This parameter measures the amount of UVA radiation reaching the Earth's surface. UVA radiation is not as harmful as UVB radiation, but it can still cause skin damage and premature aging.

4. TS (MERRA-2 Earth Skin Temperature): This parameter measures the temperature of the Earth's surface, also known as the land surface temperature (LST). LST is important for understanding a variety of environmental processes, such as energy balance, evapotranspiration, and plant growth.

5. T2M (MERRA-2 Temperature at 2 Meters): This parameter measures the air temperature at 2 meters above the ground. T2M is a widely used meteorological parameter that is used for forecasting weather, understanding

climate change, and assessing the risk of heat waves and other extreme weather events.

6. T2MDEW (MERRA-2 Dew/Frost Point at 2 Meters): This parameter measures the dew point temperature at 2 meters above the ground. The dew point temperature is the temperature at which the air must be cooled in order for water vapor to condense into dew.

7. T2M RANGE (MERRA-2 Temperature at 2 Meters Range): This parameter measures the range of air temperatures at 2 meters above the ground over a given period of time. T2M RANGE is a useful indicator of temperature variability, which can be important for understanding climate change and its impacts.

8. PRECTOTCORR (MERRA-2 Precipitation Corrected): This parameter measures the total precipitation (rain and snow) that falls on the Earth's surface over a given period of time. Precipitation is a key component of the water cycle and is important for agriculture, water resources management, and natural hazard forecasting.

9. QV2M (MERRA-2 Specific Humidity at 2 Meters): This parameter measures the amount of water vapor in the air at 2 meters above the ground. Specific humidity is a measure of the water vapor content of the air relative to the air temperature.

10. PS (MERRA-2 Surface Pressure): This parameter measures the atmospheric pressure at the Earth's surface. Surface pressure is important for understanding a variety of atmospheric processes, such as weather forecasting and climate change.

11. WS10M RANGE (MERRA-2 Wind Speed at 10 Meters Range): This parameter measures the range of wind speeds at 10 meters above the ground over a given period of time. WS10M RANGE is a useful indicator of wind variability, which can be important for understanding climate change and its impacts.

12. WS2M (MERRA-2 Wind Speed at 2 Meters): This parameter measures the wind speed at 2 meters above the ground. WS2M is a widely used meteorological parameter that is used for forecasting weather, understanding climate change, and assessing the risk of wind storms and other extreme weather events.

13. WS2M_RANGE (MERRA-2 Wind Speed at 2 Meters Range): This parameter measures the range of wind speeds at 2 meters above the ground over a given period of time. WS2M RANGE is a useful indicator of wind variability, which can be important for understanding climate change and its impacts.

Chapter – 5
RESULTS AND DISCUSSION

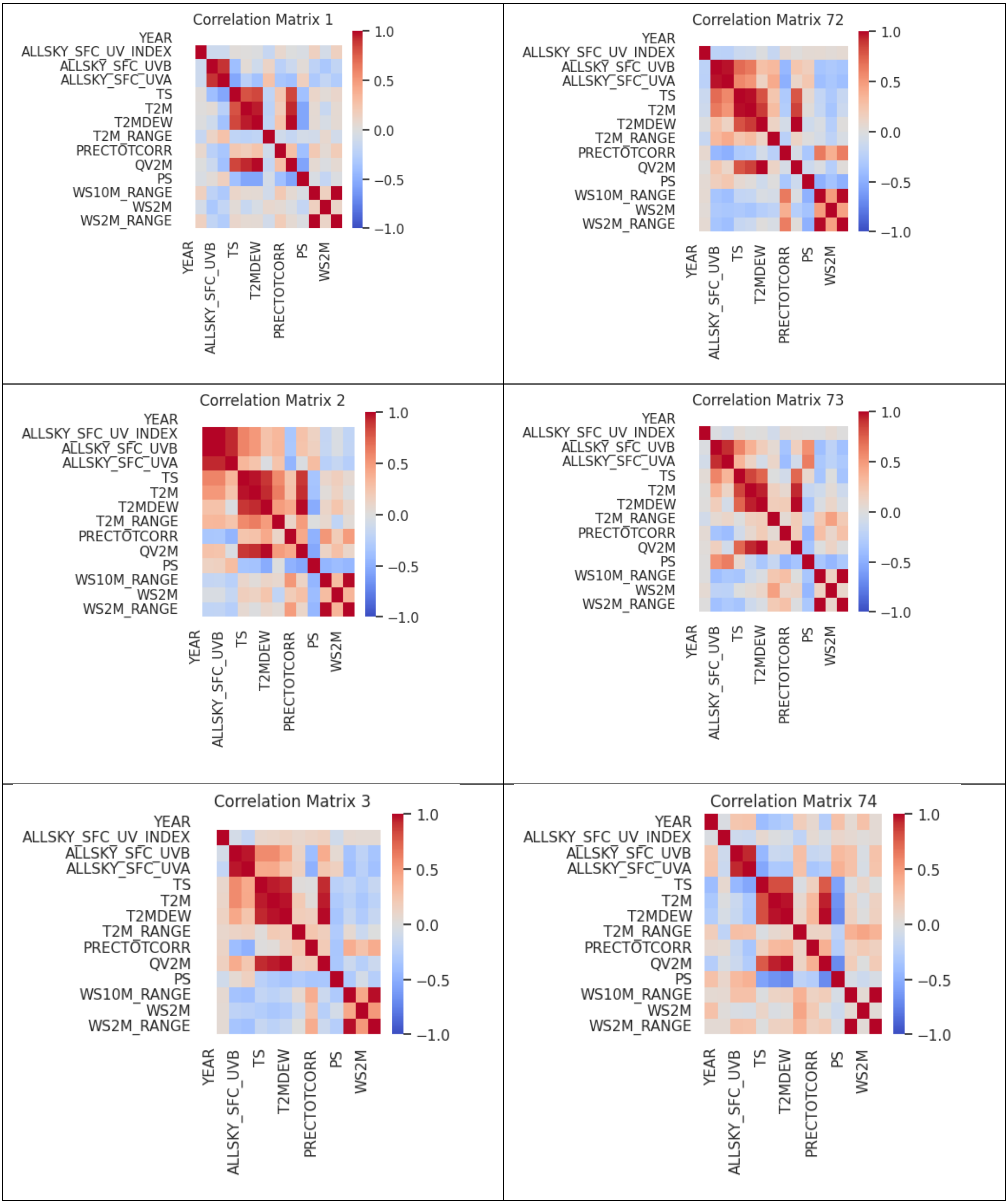

Fig. 1 Chicago

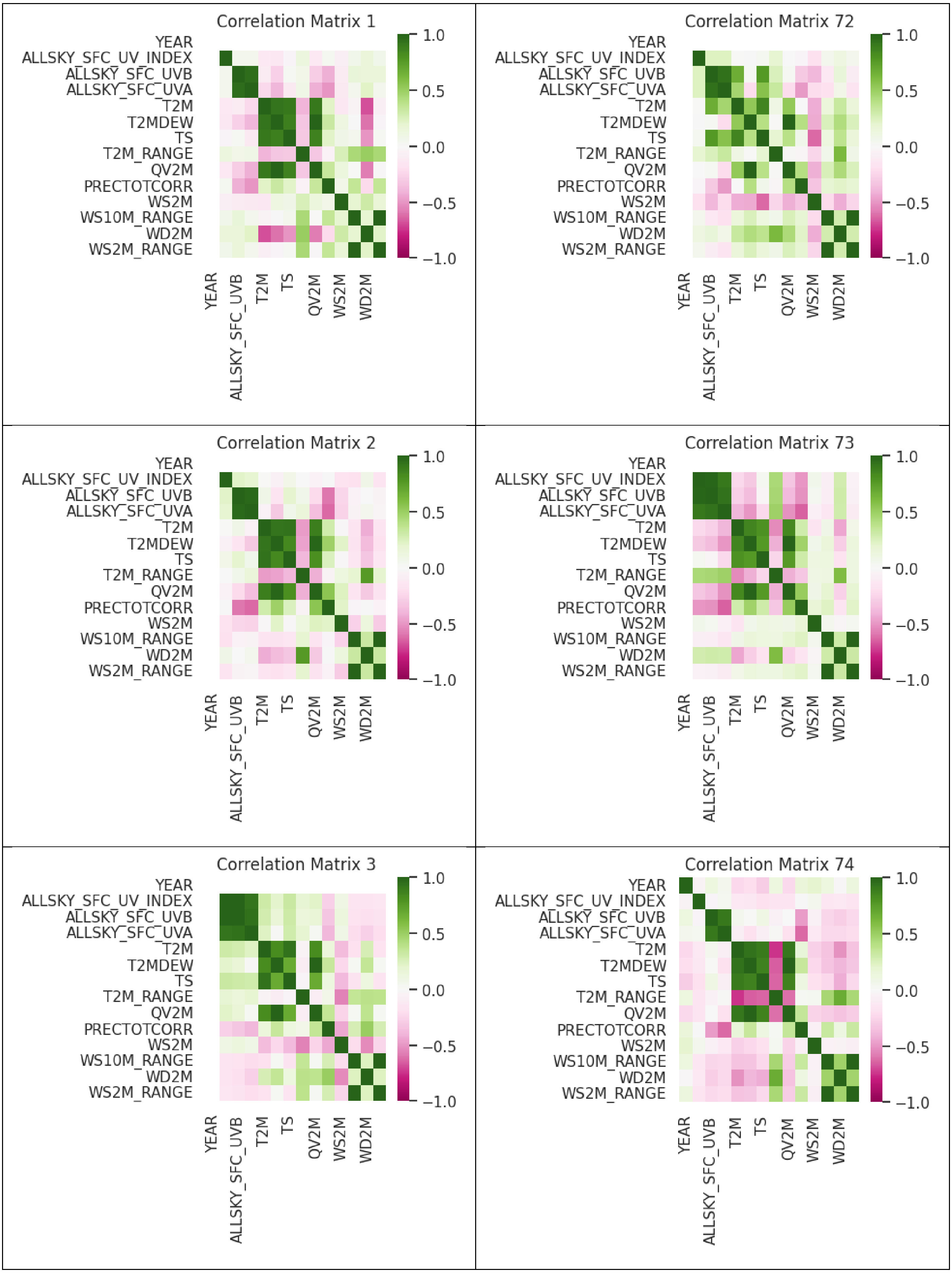
Correlation Matrix 1
Correlation Matrix 72
Correlation Matrix 2
Correlation Matrix 73
Correlation Matrix 3
Correlation Matrix 74
YEAR
ALLSKY_SFC_UV_INDEX
ALLSKY_SFC_UVB
ALLSKY_SFC_UVA
T2M
T2MDEW
TS
T2M_RANGE
QV2M
PRECTOTCORR
WS2M
WS10M_RANGE
WD2M
WS2M_RANGE
1.0
0.5
0.0
−0.5
−1.0

Fig. 2 Miami

Inference: The code analyses Fig.1 and Fig.2 Earth power data for Chicago from 2010 to 2022 by calculating cross-correlation matrices for two-month rolling windows. The resulting heatmaps visually represent the strength and direction of correlations between various parameters. High positive or negative values indicate strong associations, while values near zero suggest weak or no correlation. Examining these patterns across different time windows allows for the identification of consistent correlation trends or changes, potentially highlighting seasonal variations or anomalies. By investigating correlations between specific parameters, dependencies, and influences between them can be revealed. In summary, the analysis aims to uncover temporal patterns and relationships in Chicago's Earth power data, offering insights into the dynamic interactions among different factors over the specified timeframe.

<u>Distance between correlational matrices-</u>

```
Frame 1 to Frame 2 Distance: 0.23745820415868804
Frame 2 to Frame 3 Distance: 0.21612926602924878
Frame 3 to Frame 4 Distance: 0.271229305580888
Frame 4 to Frame 5 Distance: 0.22643900980595796
Frame 5 to Frame 6 Distance: 0.18757351123130026
Frame 6 to Frame 7 Distance: 0.22511729282802534
Frame 7 to Frame 8 Distance: 0.2513358746053793
Frame 8 to Frame 9 Distance: 0.16702982330419652
Frame 9 to Frame 10 Distance: 0.2046254342512101
Frame 10 to Frame 11 Distance: 0.21552060246379431
Frame 11 to Frame 12 Distance: 0.27410060852901424
Frame 12 to Frame 13 Distance: 0.1798045687479549
Frame 13 to Frame 14 Distance: 0.1726176824860744
Frame 14 to Frame 15 Distance: 0.15363511712703823
Frame 15 to Frame 16 Distance: 0.16009775547022925
Frame 16 to Frame 17 Distance: 0.1505821428522804
Frame 17 to Frame 18 Distance: 0.19846984968430184
Frame 18 to Frame 19 Distance: 0.24181079254427376
Frame 19 to Frame 20 Distance: 0.23494484349632946
Frame 20 to Frame 21 Distance: 0.16521853127369995
Frame 21 to Frame 22 Distance: 0.17259890247588364
Frame 22 to Frame 23 Distance: 0.1728808797414295
```

```
Frame 53 to Frame 54 Distance: 0.26829082345646665
Frame 54 to Frame 55 Distance: 0.19377105978320502
Frame 55 to Frame 56 Distance: 0.24122877621497157
Frame 56 to Frame 57 Distance: 0.18023967012791703
Frame 57 to Frame 58 Distance: 0.2553721832095551
Frame 58 to Frame 59 Distance: 0.25136944918302484
Frame 59 to Frame 60 Distance: 0.26824460613097667
Frame 60 to Frame 61 Distance: 0.24127824477502793
Frame 61 to Frame 62 Distance: 0.27978217793574883
Frame 62 to Frame 63 Distance: 0.18114461906198162
Frame 63 to Frame 64 Distance: 0.2562341703631459
Frame 64 to Frame 65 Distance: 0.21129848486486114
Frame 65 to Frame 66 Distance: 0.20911698795438696
Frame 66 to Frame 67 Distance: 0.2687400664914542
Frame 67 to Frame 68 Distance: 0.20169947968095833
Frame 68 to Frame 69 Distance: 0.1624199561345702
Frame 69 to Frame 70 Distance: 0.14404329311742514
Frame 70 to Frame 71 Distance: 0.24668090641213997
Frame 71 to Frame 72 Distance: 0.19373250617388318
Frame 72 to Frame 73 Distance: 0.17787177318028427
Frame 73 to Frame 74 Distance: 0.2373065178420879
Frame 74 to Frame 75 Distance: nan
```

Fig. 3 Chicago

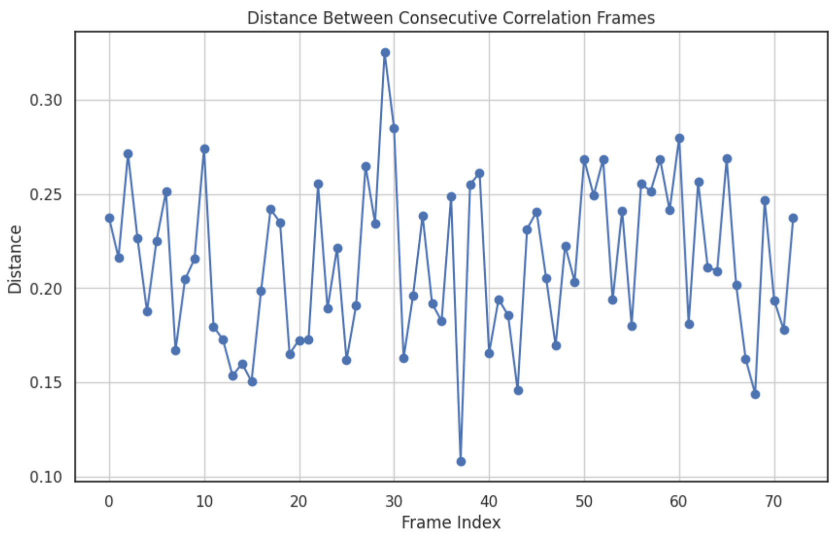

Fig. 4 Chicago

```
Frame 1 to Frame 2 Distance: 0.17269654787930694
Frame 2 to Frame 3 Distance: 0.21350897526029192
Frame 3 to Frame 4 Distance: 0.23561481876620757
Frame 4 to Frame 5 Distance: 0.25825161488552795
Frame 5 to Frame 6 Distance: 0.2579135050886714
Frame 6 to Frame 7 Distance: 0.18092011953219816
Frame 7 to Frame 8 Distance: 0.20478983879495177
Frame 8 to Frame 9 Distance: 0.22838483944198076
Frame 9 to Frame 10 Distance: 0.30239082142823737
Frame 10 to Frame 11 Distance: 0.2568021452598674
Frame 11 to Frame 12 Distance: 0.24919352952737722
Frame 12 to Frame 13 Distance: 0.17965131174036
Frame 13 to Frame 14 Distance: 0.23625273960476623
Frame 14 to Frame 15 Distance: 0.1877838048305784
Frame 15 to Frame 16 Distance: 0.19556635176015721
Frame 16 to Frame 17 Distance: 0.32883420098370436
Frame 17 to Frame 18 Distance: 0.28538633854751355
Frame 18 to Frame 19 Distance: 0.16819485705080825
Frame 19 to Frame 20 Distance: 0.24823747317785252
Frame 20 to Frame 21 Distance: 0.18614089836143127
Frame 21 to Frame 22 Distance: 0.24728315948996912
Frame 22 to Frame 23 Distance: 0.2862297429850601
```

```
Frame 52 to Frame 53 Distance: 0.29168040808690027
Frame 53 to Frame 54 Distance: 0.1808046497112061
Frame 54 to Frame 55 Distance: 0.1576005370276472
Frame 55 to Frame 56 Distance: 0.19357955026430557
Frame 56 to Frame 57 Distance: 0.25129882504584705
Frame 57 to Frame 58 Distance: 0.21645408230519994
Frame 58 to Frame 59 Distance: 0.23986086412356028
Frame 59 to Frame 60 Distance: 0.2191231484718267
Frame 60 to Frame 61 Distance: 0.1822382263924133
Frame 61 to Frame 62 Distance: 0.31134290300146655
Frame 62 to Frame 63 Distance: 0.2611823124664322
Frame 63 to Frame 64 Distance: 0.2781059289061353
Frame 64 to Frame 65 Distance: 0.23803790757581875
Frame 65 to Frame 66 Distance: 0.29272366943665823
Frame 66 to Frame 67 Distance: 0.19701657122690275
Frame 67 to Frame 68 Distance: 0.22627021830585986
Frame 68 to Frame 69 Distance: 0.1720335968546856
Frame 69 to Frame 70 Distance: 0.28580427892276156
Frame 70 to Frame 71 Distance: 0.24048842619127017
Frame 71 to Frame 72 Distance: 0.2539130515099964
Frame 72 to Frame 73 Distance: 0.2219955090302923
Frame 73 to Frame 74 Distance: 0.11507963237208388
```

Fig. 5 Miami

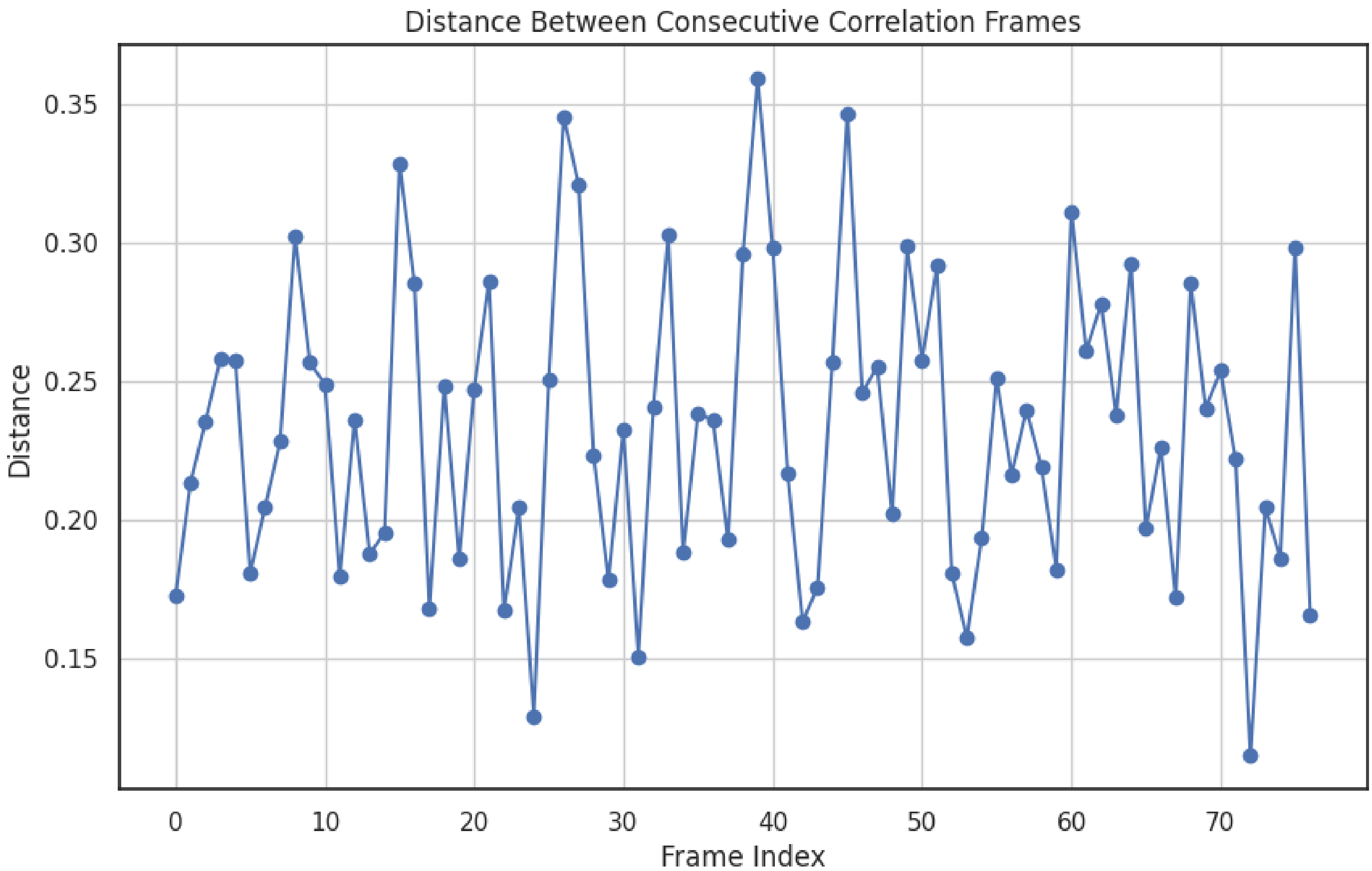

Fig. 6 Miami

Inferences: From this Fig.3,4,5,6 . we infer how different Earth power measurements in Chicago change over time from 2010 to 2022. It happens by checking how much the relationships between these measurements shift every two months. The code calculates the distance between these shifts and shows the results in a graph. Peaks in the graph point to times when things change a lot, and valleys show more stable periods. Big distances mean significant changes in the relationships between measurements, while small distances mean things stay more consistent. This helps us spot when and how the connections between these Earth power factors evolve over the years, offering insights into how the environment in Chicago changes seasonally or due to specific events.

<u>**Average Matrix of corelation frames-**</u>

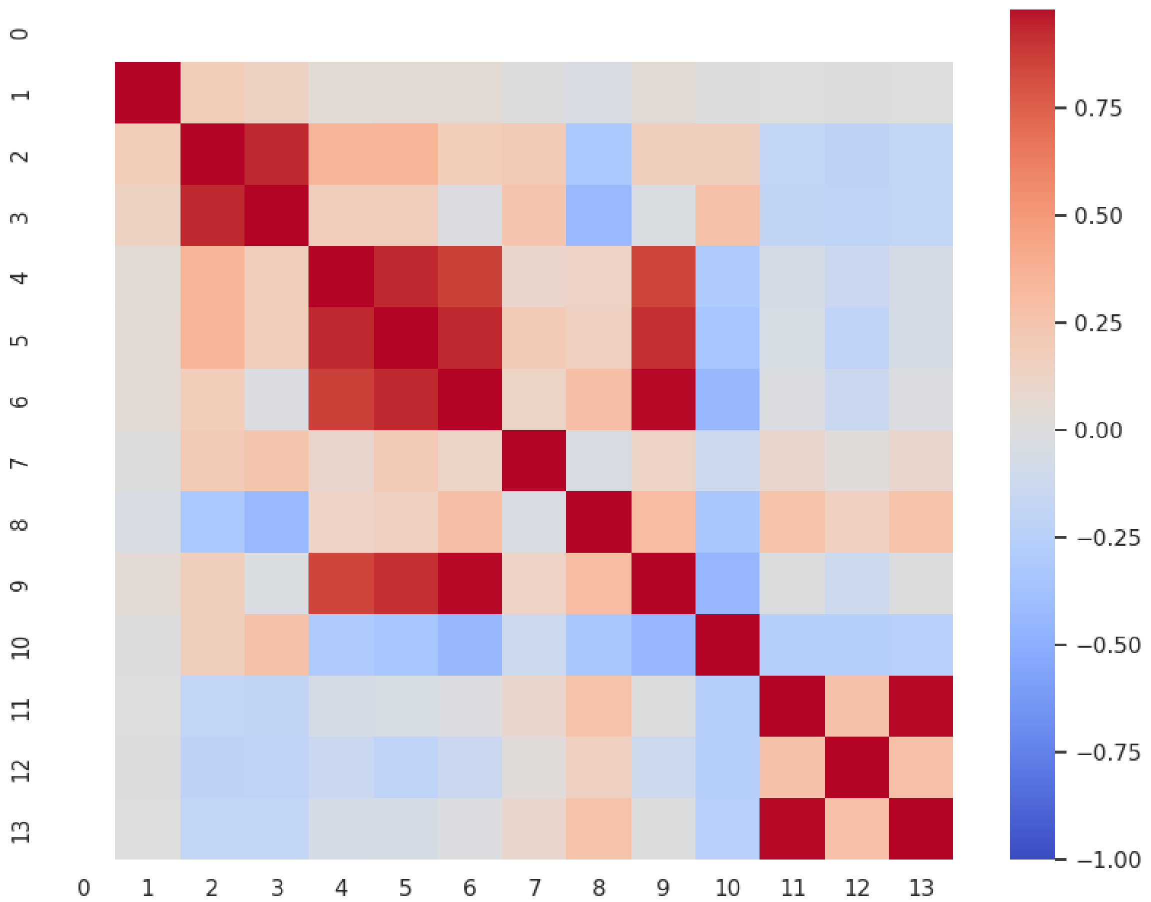

Fig. 7 Chicago

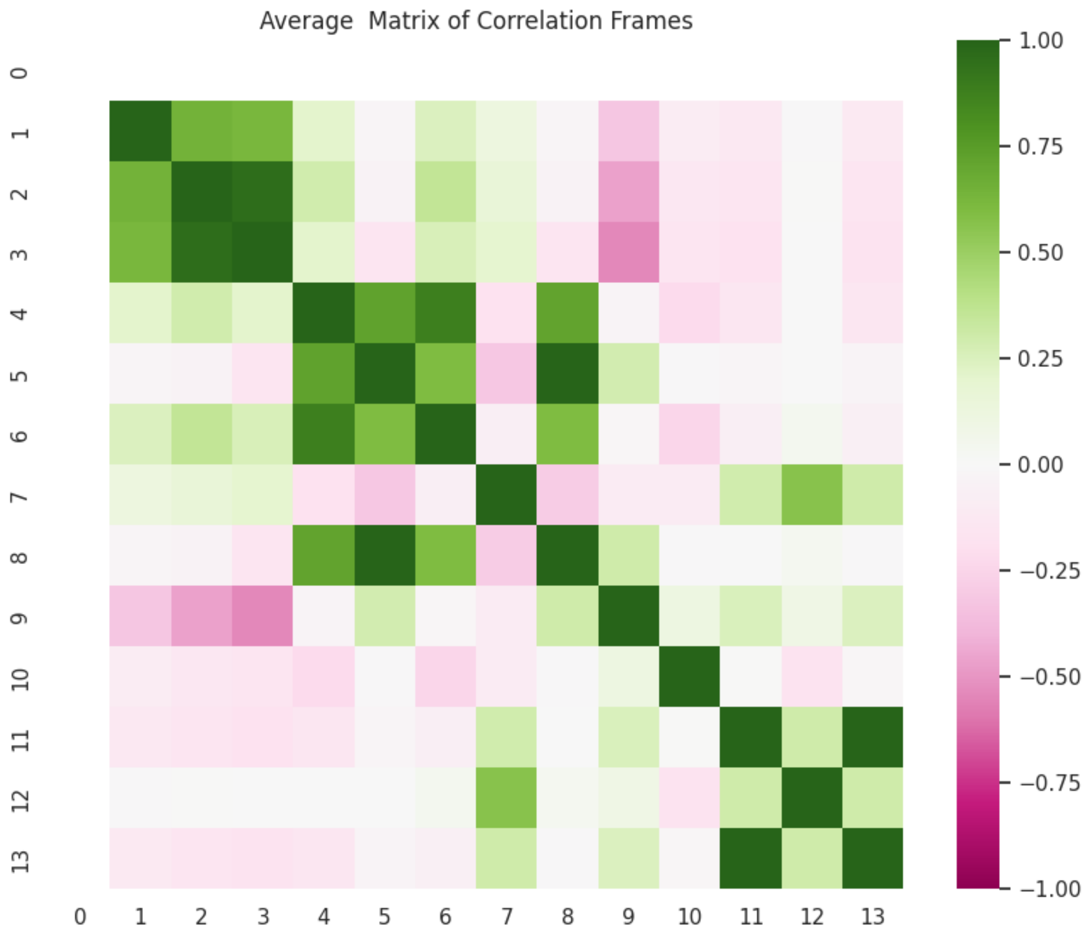

Fig. 8 Miami

Inferences:

It (in Fig.7 and Fig.8) calculates rolling cross-correlation matrices for two-month windows and then computes the average similarity matrix by taking the mean of these matrices. The resulting heatmap reveals the average correlation patterns among various Earth power parameters over the specified time frame. Darker shades indicate stronger correlations, while lighter shades suggest weaker or opposite correlations. This consolidated view provides insights into the overall trends and relationships within the Earth power data.

Density and time series plot for UVB radiation from2010 to 2022:

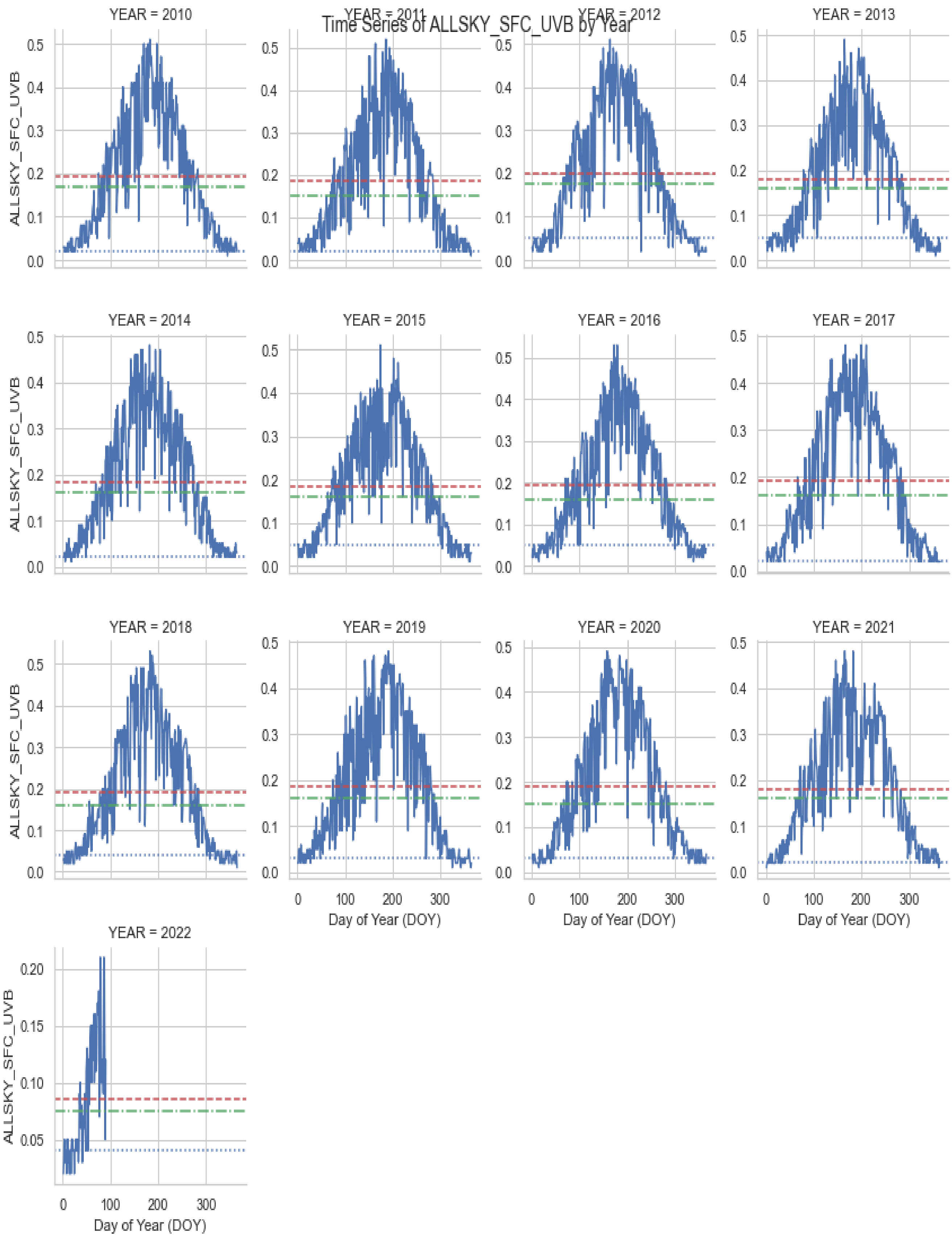

Fig. 9 Chicago

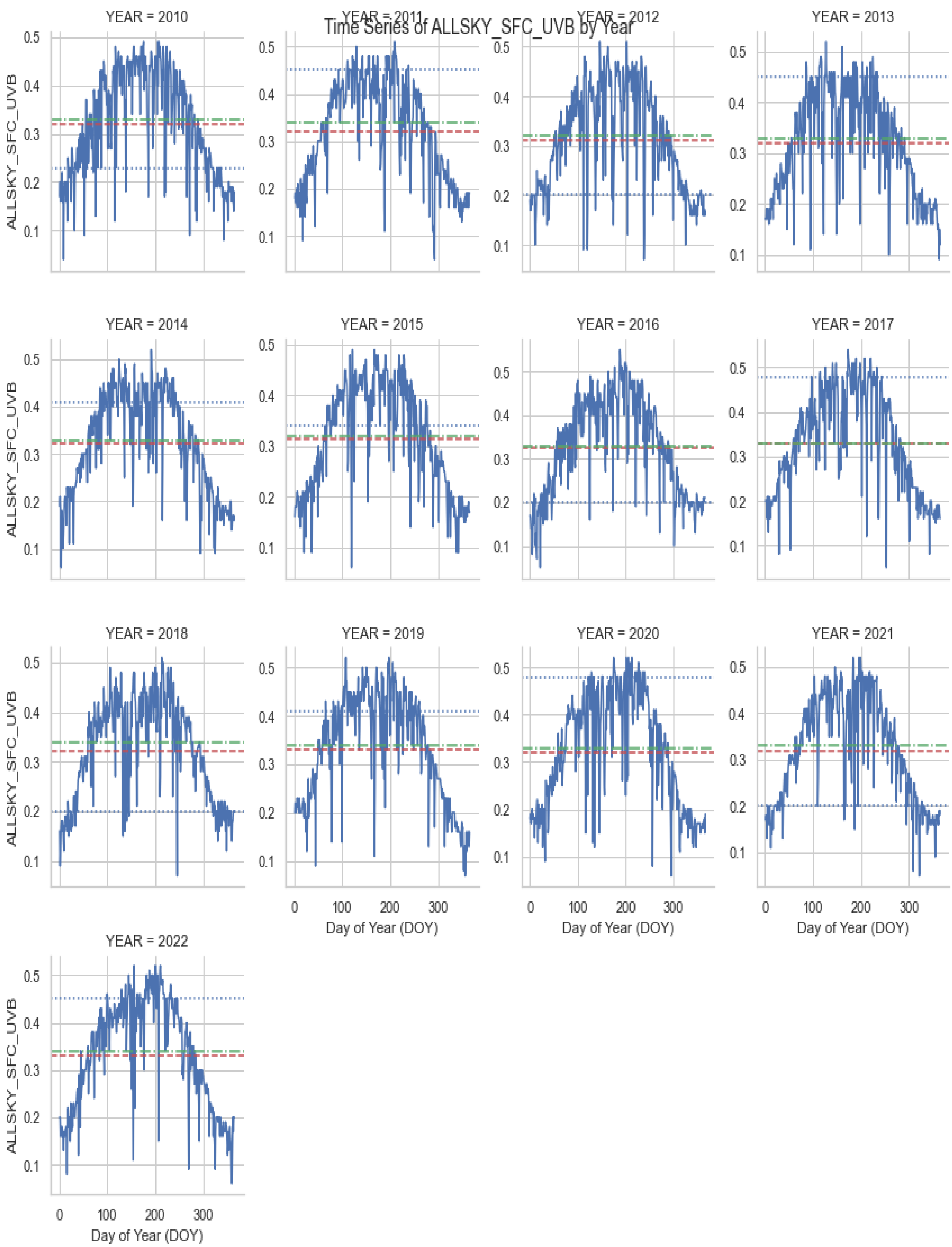
Time Series of ALLSKY_SFC_UVB by Year
YEAR = 2010
YEAR = 2011
YEAR = 2012
YEAR = 2013
YEAR = 2014
YEAR = 2015
YEAR = 2016
YEAR = 2017
YEAR = 2018
YEAR = 2019
YEAR = 2020
YEAR = 2021
YEAR = 2022
ALLSKY_SFC_UVB
Day of Year (DOY)

Fig. 10 Miami

Inferences:

Combining the insights from the two graphs Fig.9 and Fig.10 offers a holistic understanding of the "ALLSKY_SFC_UVB" parameter in the dataset. The density plot, organized by year, provides an overview of the distribution patterns, aiding in the identification of any significant shifts or trends over the years. Simultaneously, the time series plot, delves into the temporal dynamics of "ALLSKY_SFC_UVB," highlighting variations within specific groups. This dual perspective enables a nuanced exploration, where the density plot captures annual trends, and the time series plot with clusters allows for a more detailed examination of distinct temporal patterns within each cluster. Together, these visualizations offer a comprehensive depiction of the parameter's distribution and behaviour, facilitating a richer interpretation of the Earth power data.

<u>Fuzzy c-means clustering and heat map for Earth skin temperature vs UVB radiation:</u>

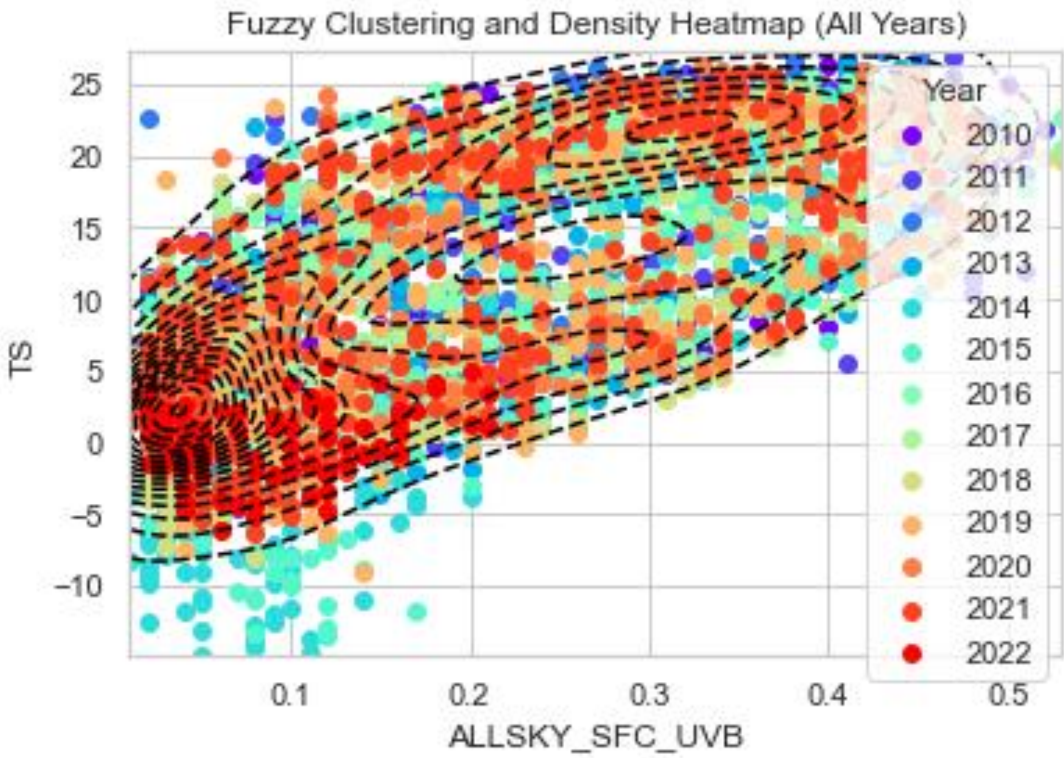

Fig. 11 Chicago

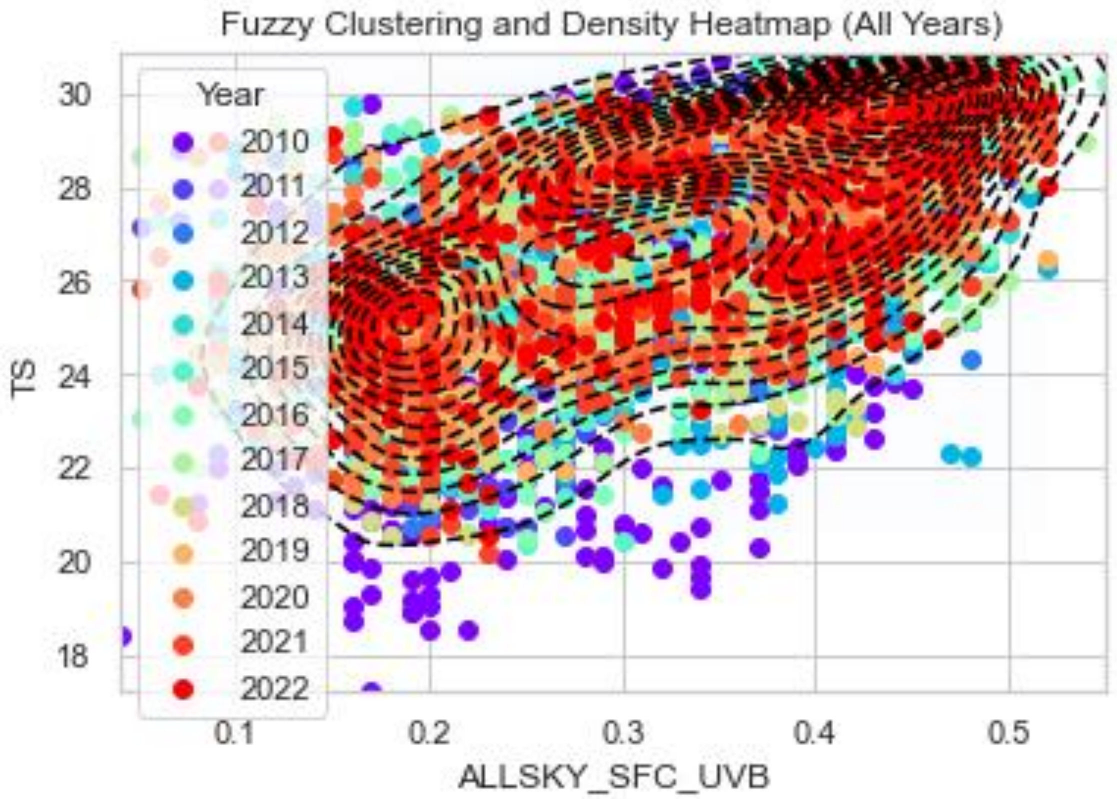

Fig. 12 Miami

Inferences:

In the generated plot Fig.11 and Fig.12, the relationship between "ALLSKY_SFC_UVB" and "TS" parameters across multiple years is visually depicted. The scatter plot, color-coded by each year, reveals fluctuations in the interplay between these two factors. Notably, the density heatmap highlights regions where data points are densely concentrated, emphasizing areas of significant activity. Examining the contour lines provides additional clarity on the density levels, aiding in the identification of specific patterns. Changes in the distribution of data points over the years become apparent, showcasing how "ALLSKY_SFC_UVB" and "TS" vary together.

Joint regression plot between earth skin temperature and temperature at 2M range:

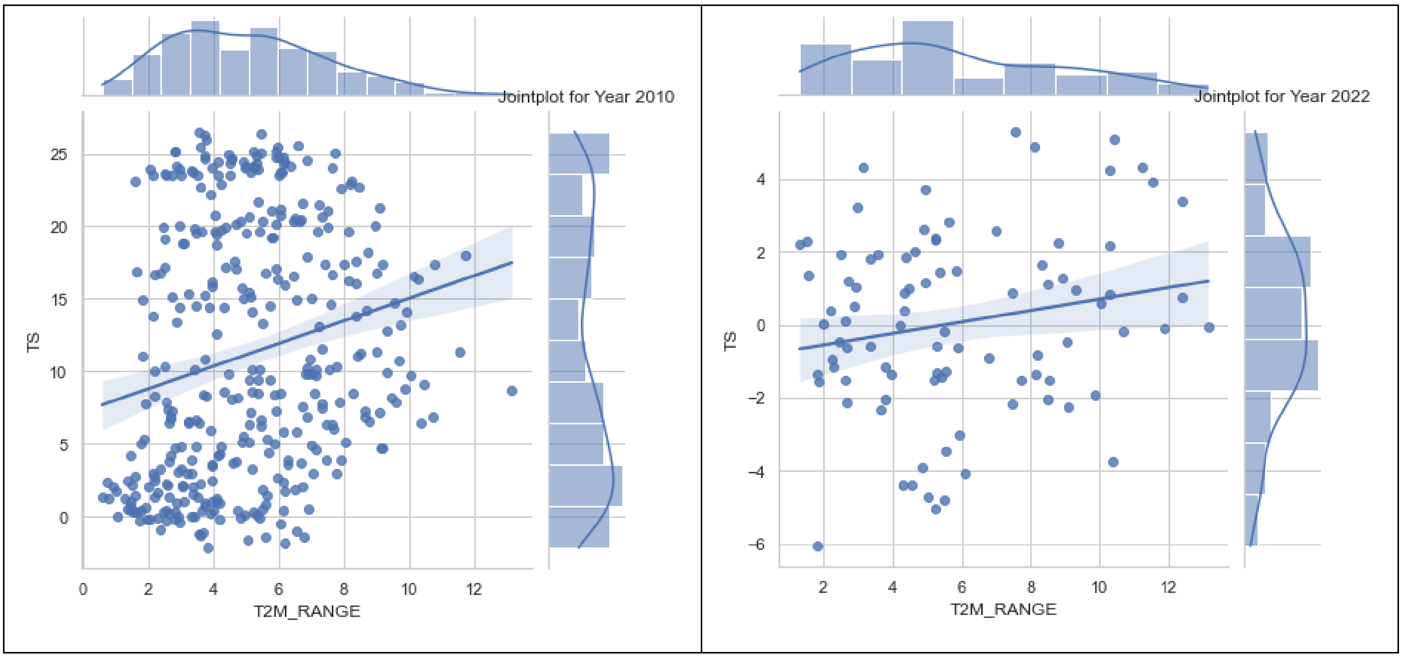

Fig. 13 Chicago

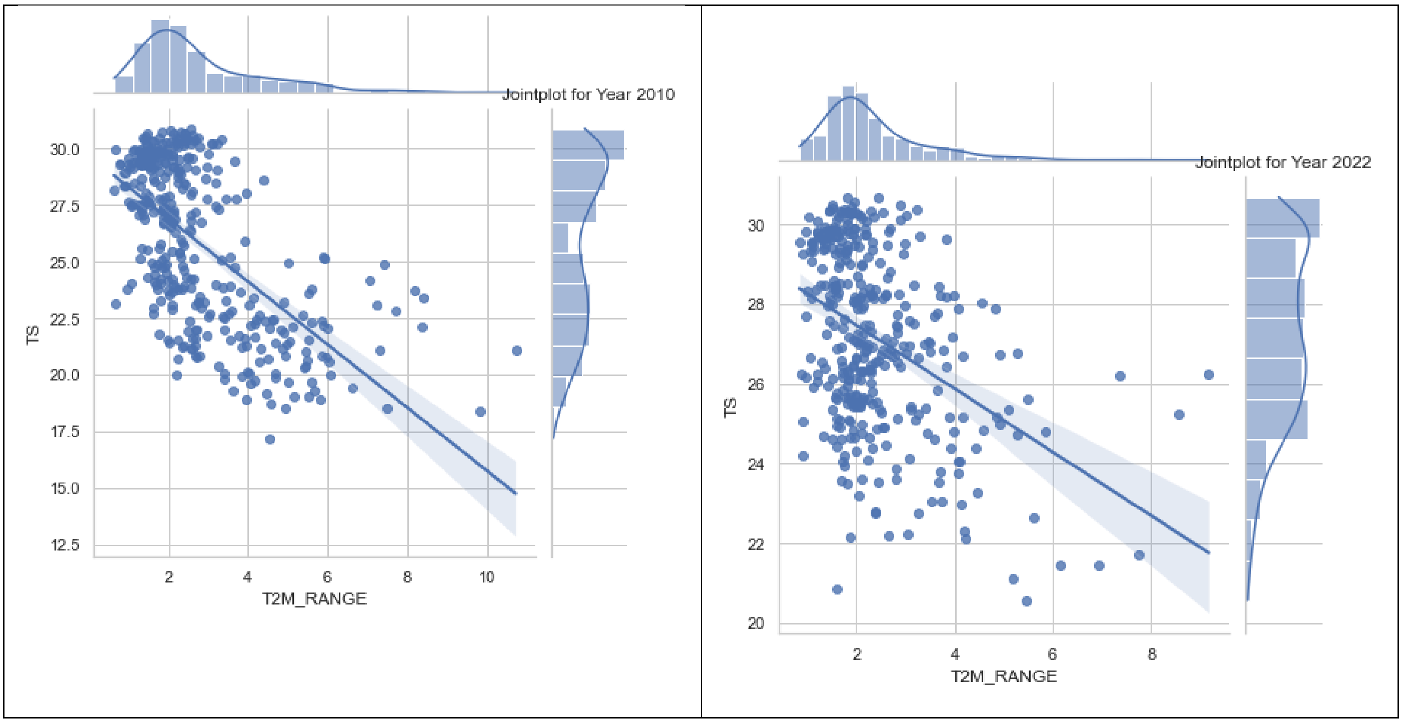

Fig. 14 Miami

Inferences:

The series of joint plots Fig.13 and Fig.14 generated by the provided Python code offer insights into the relationship between 'T2M_RANGE' (temperature range) and 'TS' (surface temperature) parameters across the years 2010 to 2022. Each plot provides a visual representation of the correlation between these two variables for a specific year, featuring a scatter plot and a regression line. The inclination and pattern of the regression lines across different years indicate the nature and strength of the association. Observing these plots collectively allows us to infer trends and variations in the correlation between temperature range and surface temperature over the specified timeframe. For instance, consistent upward or downward trends in the regression lines may suggest a continuous relationship, while varying patterns could indicate seasonal or temporal fluctuations in the association between the parameters.

Relationship between UVB radiation and temperature at 2M range using density plot:

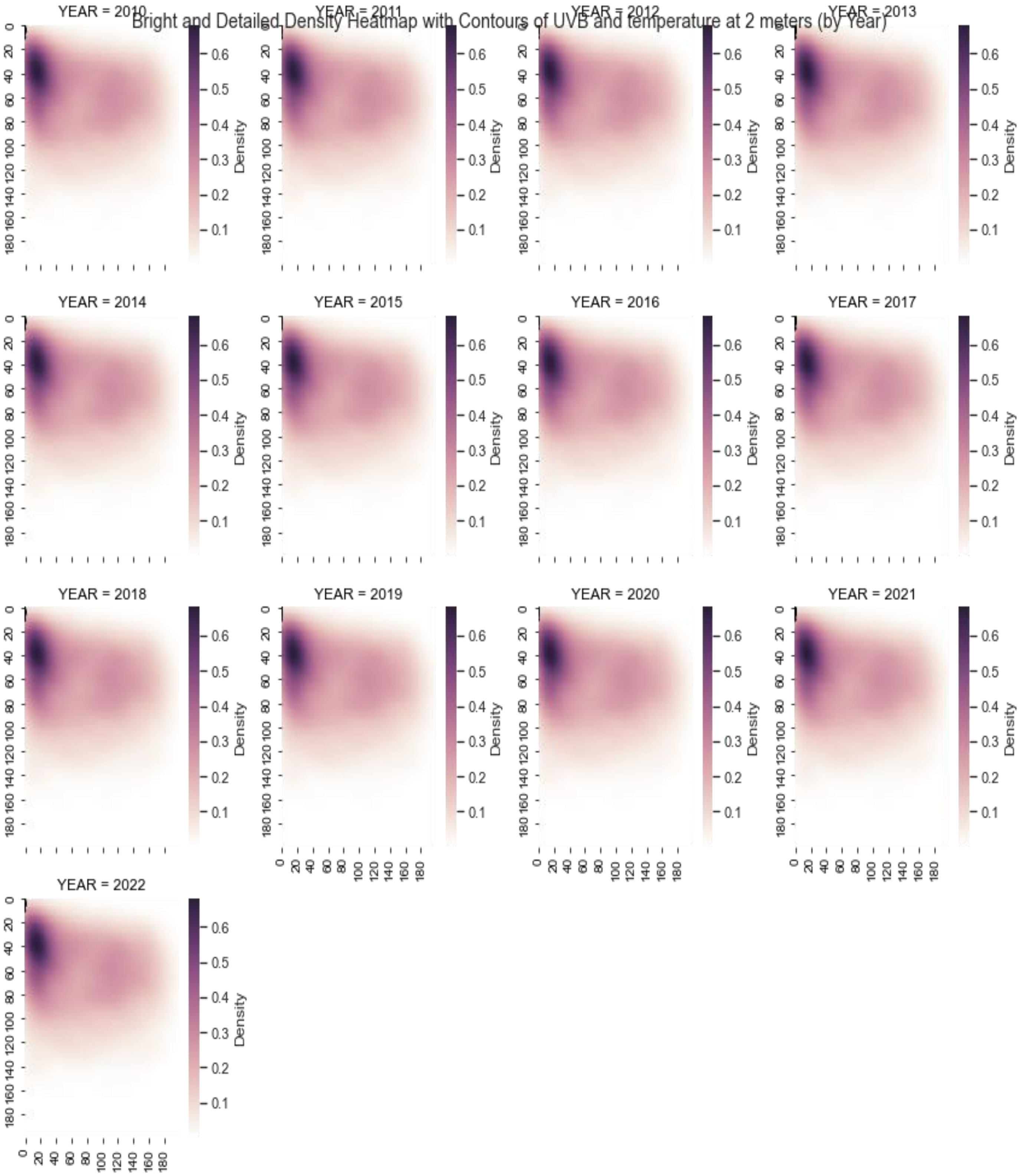

Fig. 15 Chicago

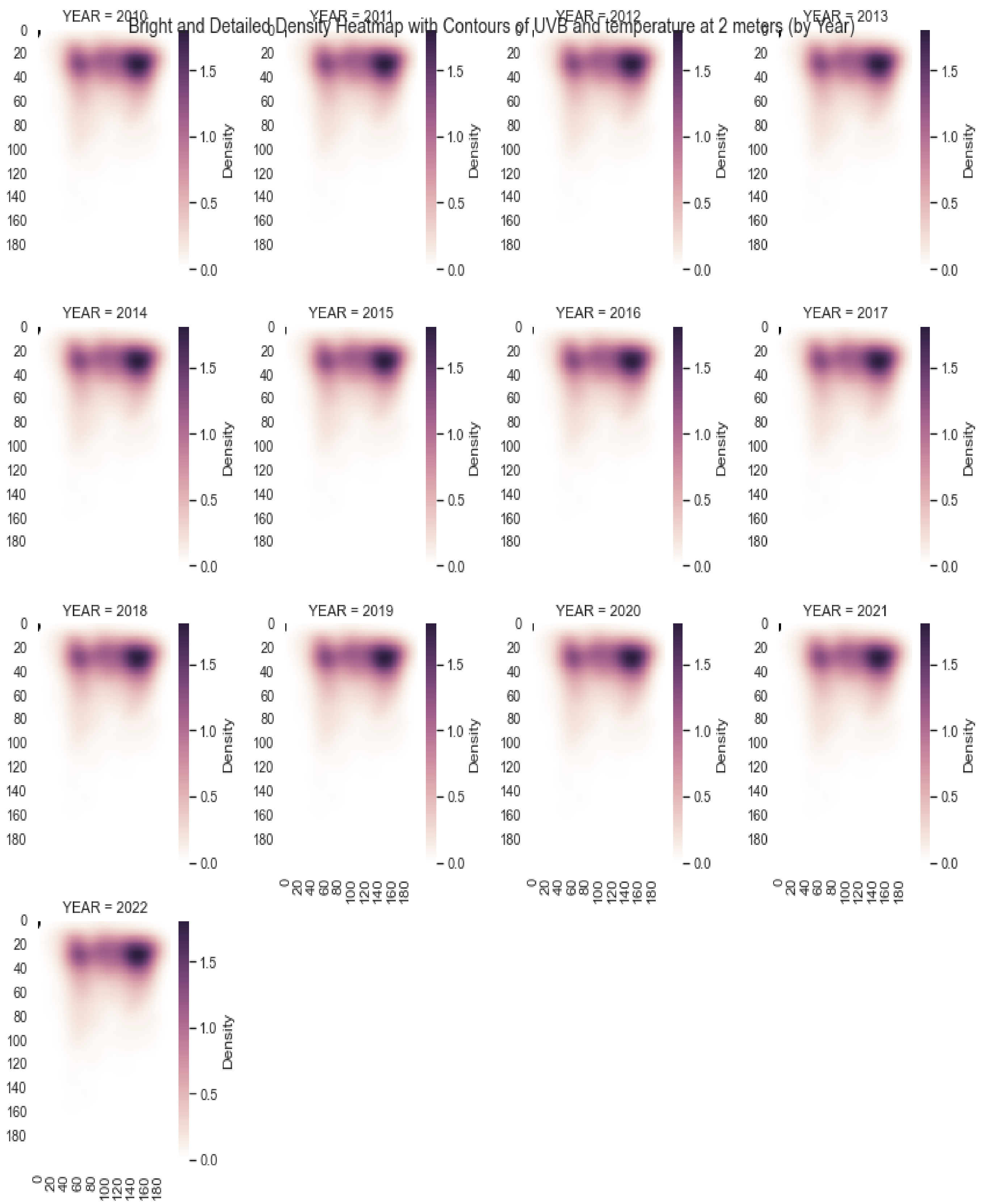
Bright and Detailed Density Heatmap with Contours of UVB and temperature at 2 meters (by Year)
YEAR = 2010
YEAR = 2011
YEAR = 2012
YEAR = 2013
YEAR = 2014
YEAR = 2015
YEAR = 2016
YEAR = 2017
YEAR = 2018
YEAR = 2019
YEAR = 2020
YEAR = 2021
YEAR = 2022
Density

Fig. 16 Miami

Inferences:

The Python code in Fig.15 and Fig.16 generates a series of bright and detailed density heatmaps with contours, showcasing the distribution patterns of "ALLSKY_SFC_UVB" and "T2M_RANGE" parameters across multiple years (2010 to 2022). Utilizing fuzzy clustering, each data point is assigned a cluster label, enabling the observation of distinct clusters within the heatmaps. The heatmaps vividly depict areas of higher data concentration, while contours provide additional details about density levels. This comprehensive visualization, organized by year, facilitates the identification of trends and variations in the relationship between UVB intensity and temperature range over time. The contour lines further enhance the delineation of density patterns, offering a nuanced exploration of the Earth power dataset.

Standard Deviation Plot (Z-Test) :

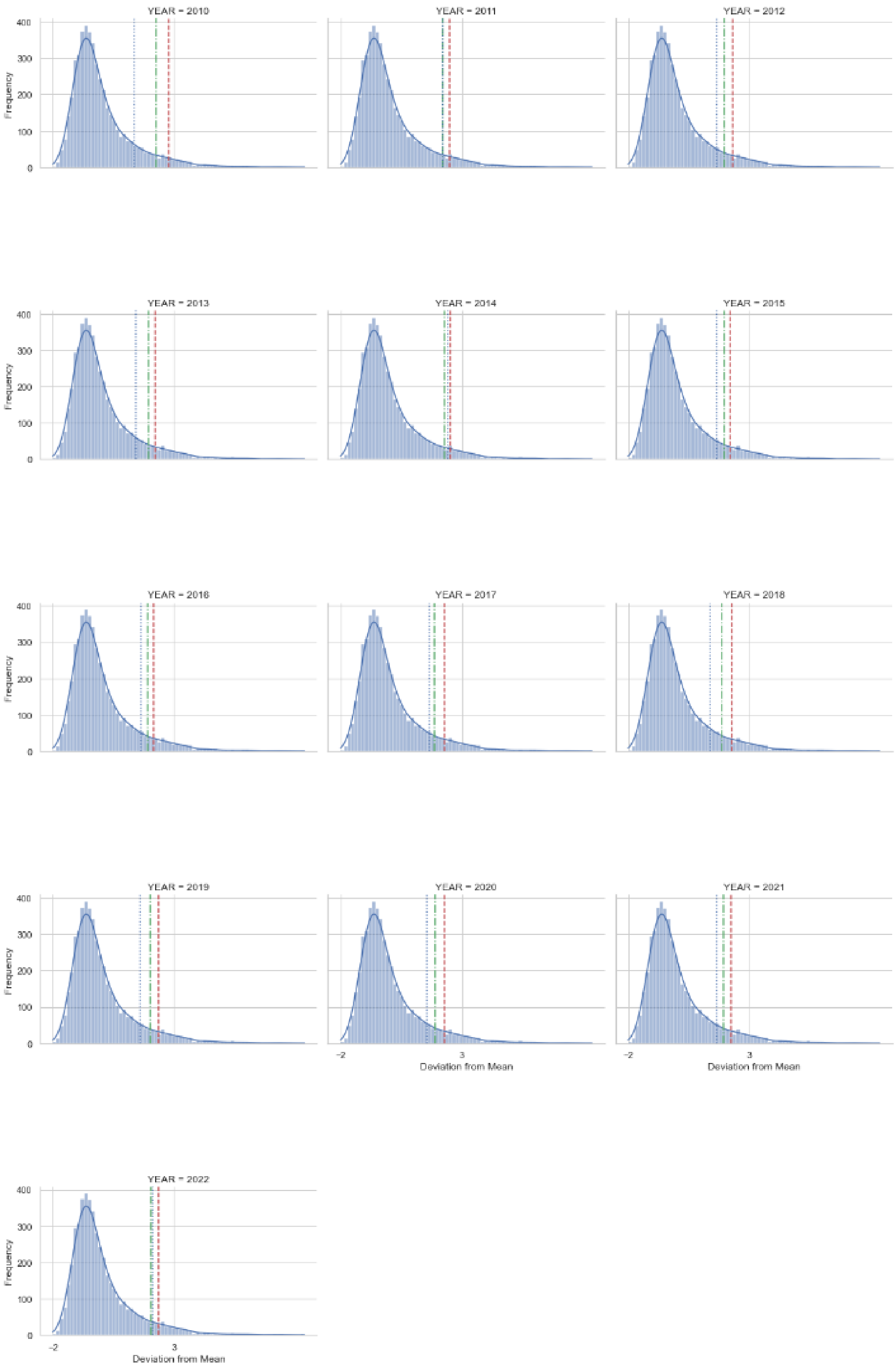

Fig. 17 Miami

Inferences:

The generated plot Fig.17 , employing histograms with Kernel Density Estimates (KDE) overlaid in a FacetGrid configuration for each year, illustrates the distributional characteristics of deviations from the mean for the 'T2M_RANGE' variable across temporal dimensions. The inclusion of red dashed lines denoting the mean, green dash-dot lines indicating the median, and blue dotted lines representing the mode facilitates a nuanced analysis of central tendency and distributional shifts over the years. An examination of these metrics provides insights into the variability and systematic trends in temperature deviations, aiding in the identification of potential changes in the underlying climatic patterns. The visualization is particularly adept at discerning alterations in both the central location and spread of the deviation distribution, contributing to a more granular understanding of the dataset's temporal dynamics.

Chapter – 6
FUTURE OUTLOOK

As we extend our investigation into the impacts of climate change on both Chicago and Miami over the past 13 years, We go beyond temperature and UV radiation. Increasing our scope, we could conduct a more thorough analysis that includes important meteorological factors like wind, humidity, dew point, and precipitation.

The goal of this expanded analytical method is to provide a comprehensive picture of how the climates in Miami and Chicago are changing. Through an in-depth examination of wind patterns, humidity variations, dew points, and precipitation dynamics, we hope to reveal a complex story that clarifies the various elements influencing the environmental composition of both cities.

Our goal remains the same: to extract meaningful insights using strong data analysis and visualization strategies, similar to our previous approaches with regard to temperature and UV radiation. These observations are meant to serve as fundamental cornerstones for well-informed decision-making, creative approaches to urban planning, and flexible solutions to the problems presented by Chicago's and Miami's changing environments.

This continued exploration is motivated by the need to comprehend how different elements of the environment are interconnected. Our goal in extending our research to these new areas in both cities is to make a substantial contribution to the conversation about the local effects of climate change. With continued exploration, we aim to offer deeper insights into the environmental histories of Chicago and Miami, empowering informed decisions for resilient and sustainable futures in both urban landscapes.

Chapter – 7
REFRENCES

Dataset Link:

Chicago

https://drive.google.com/file/d/1iA-Q-Cu0LbsosvYgXMloCDpHDaprNiNt/view?usp=drive_link

Miami

https://drive.google.com/file/d/1sTutCs8upCmD8lCRrROEPzJA6hyI6TQF/view?usp=drive_link

Data Source: https://power.larc.nasa.gov/data-access-viewer/

PAPER LINK:

[1] Orte, F., Lusi, A., Carmona, F., D'Elia, R., Faramiñán, A. and Wolfram, E., 2021, November. Comparison of NASA-POWER solar radiation data with ground-based measurements in the south of South America. In *2021 XIX Workshop on Information Processing and Control (RPIC)* (pp. 1-4). IEEE.

[2] White, J.W., Hoogenboom, G., Wilkens, P.W., Stackhouse Jr, P.W. and Hoel, J.M., 2011. Evaluation of satellite-based, modeled-derived daily solar radiation data for the continental United States. *Agronomy journal*, *103*(4), pp.1242-1251.

[3] Chandler, W.S., Hoell, J.M., Westberg, D., Whitlock, C.H., Zhang, T. and Stackhouse Jr, P.W., 2010. Near real-time global radiation and meteorology Web services available from NASA. In *Proceedings of the Solar 2010 Conference (American Solar Energy Society), May* (pp. 18-22).